CHAPTER VIII

DEVELOPMENTS IN PILOT-WIRE DIFFERENTIAL PROTECTION

8.1 INTRODUCTION :

Theoretically 'Unit' protection provides almost perfect selectivity in protecting any element in a power system. However, in the case of long transmission lines it is less effective due to the amplitude and phase angle errors introduced by the pilot link calling for the use of compensating networks[53]. Further, the cost of pilot link may not be justifiable and the voltage energization of pilot link impose limitations. When the transmission line to be protected is about 10 to 15 miles in length and pilot wires are available for other purpose, viz. telephone lines the differential pilot-wire scheme provides sufficiently good accuracy at a justifiable cost.

Rushton[54] has analysed the pilot-wire protection system on the admittance plane of pilot circuits considering the latter as a 4-terminal network. The discriminating requirements of the protection schemes are outlined from the considerations of system conditions and the effect of remote end relay characteristic on the local end is explained.

The multi-input cosine type phase comparators employed by Humpage and others[55,56], for this mode of protection suffer from the following two limitations :

(i) The unwanted line segments appearing in the 'stable zone ' of the relay introduce additional segments on the remote end relay characteristic, usually resulting in the enlargement of the area for the sequential tripping.

(ii) The measuring circuit of the relay impose special problems in obtaining the necessary signals for the phase comparison, particularly when the latter are in higher number and need mixing of system quantities.

In chapter 3 of the present work it is shown that the unwanted line segments of the characteristic on the impedance plane can be avoided by employing pulse techniques with sine type phase comparators. Further, this type of comparator provides fastest measurement of the direction. It was, therefore, thought necessary to employ sine type phase comparator for the pilot-wire differential protection system so as to over-come some of the limitations of the earlier developments.

Khincha and others[57,18], have reported the developments in amplitude comparison techniques for distance protection system where the amplitude comparison between the derived quantities is effected at every instant. The important advantages of these techniques include the need of relatively simple circuitry for the comparison and the lack of mixing of the system quantities in the formation of the necessary signals. This analysis has been further explorded in this chapter to report relaying circuitry with simple arrangements of measuring circuits.

In the present chapter, therefore, the principles of shaping of the stable zones are initially summarised. An inversion chart is included to facilitate the shaping of the stable zone. Typical stable zones are then synthesized and complete relay circuits, along with the necessary mathematical back-up, are presented both for sine type phase comparators and instantaneous amplitude comparators to obtain typical stable zones on the admittance plane of the pilot circuits.

8.2 PRINCIPLE OF THE PROTECTION SCHEME :

The essential requirement of a protection scheme is to discriminate between healthy and through fault conditions on one hand and the internal faults on the other. Unlike the distance relay analysis, the analysis of pilot-wire relays is carried out on the input admittance plane of the pilot link as it is more convenient.

As shown in Appendix, the input admittance Y_{PR} of a pilot link is given by

$$Y_{PR} = \frac{A-K\angle\delta}{B} \qquad \text{.... (8.1)}$$

Where A and B are the general line constants of the pilot circuit, the latter being considered as a 4-terminal network. Factor K is the scalar ratio of the voltages at two ends of the pilot circuit and δ is the angular difference between them.

Fig.8.1 shows the variation of K and δ on the admittance plane of a typical pilot circuit[54]. The point $K = 1$; $\delta = 0$ represents the ideal unfaulted condition. There exists a small ' stable zone ' for through faults and unfaulted conditions. The tripping should be ineffective inside this zone and should be effective for the rest of the plane. This zone may be circular, quadrilateral or of any well defined shape and must enclose the point $K = 1$; $\delta = 0$ well within.

In a differential protection scheme, the currents of the local and remote ends are compared in a comparator, the current from the remote end being obtained by means of the pilot circuits. Fig.8.2 illustrates the schematic arrangement of a typical pilot-wire differential protection system. Summation transformers are employed to obtain a single phase quantity from the 3-phase quantity for the transmission over the two wire pilot link. The comparator employed should have a blocking sense inside the stable zone. The shape of the stable zone will depend upon the voltages on the two ends, physical dimensions of the pilot link, etc.

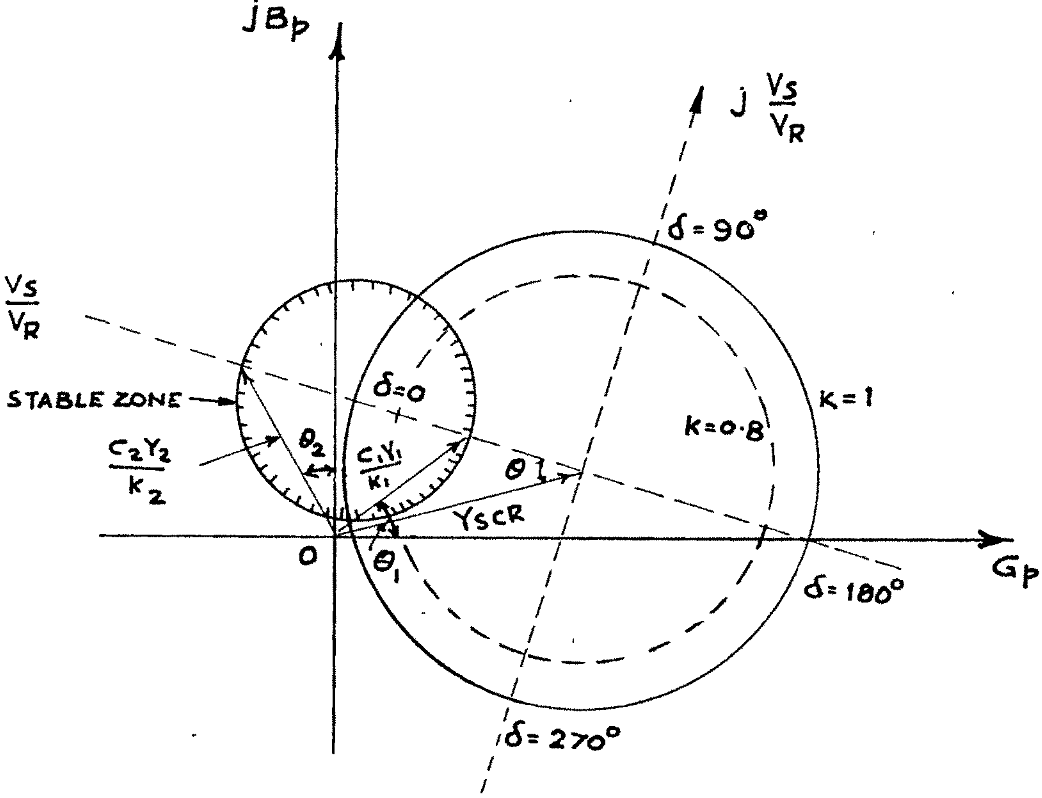

FIG. 8·1 VARIATION OF K AND δ ON ADMITTANCE PLANE

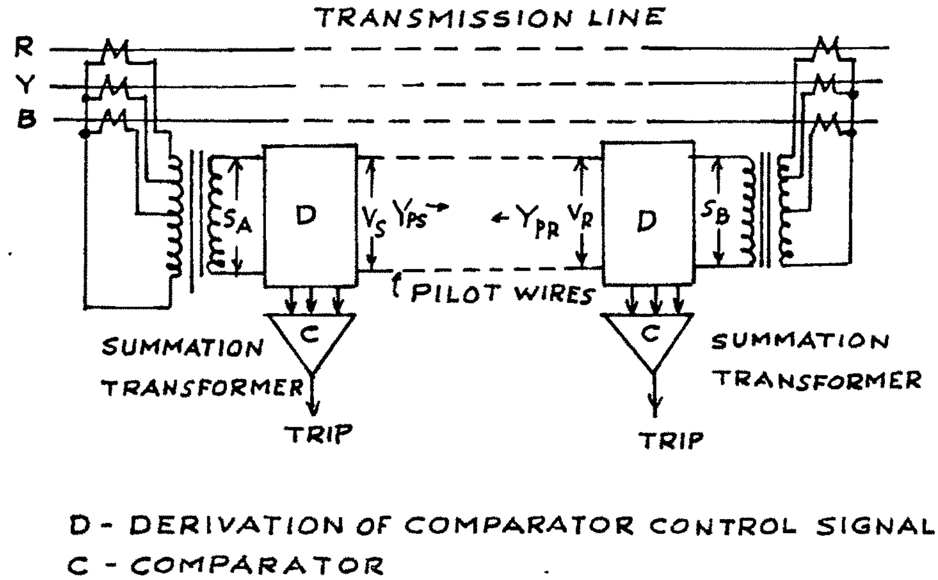

FIG. 8·2 SCHEMATIC DIAGRAM OF PROTECTION SCHEME

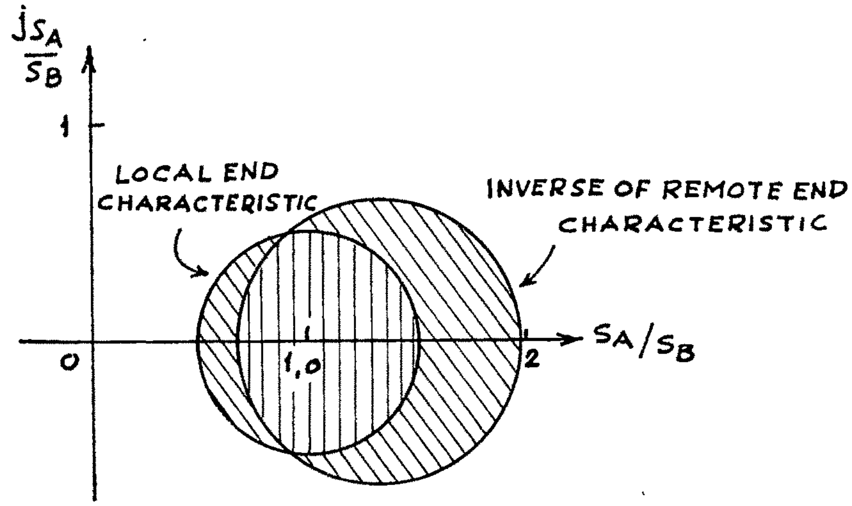

FIG. 8·3 PLANE OF THE RATIO OF RELAYING SIGNALS

Further, for the simultaneous tripping of the breakers on the two ends of the line, the common tripping region of the local end relay characteristic and the inverse of the remote end relay characteristic should be as large as possible, without sacrificing the coverage of the stable zone.

8.3 CHOICE OF STABLE ZONE :

To determine the adequate shape of the stable zone, the procedure outlined below is required to be followed :

As a first step, the curves of the variations of K and δ are required to be plotted on the input admittance plane of the pilot link as shown in fig.8.1. The point $K = 1$; $\delta = 0$ represents the ideal unfaulted condition. From this point, an axis V_S / V_R is drawn which passes through the tip of the vector Y_{SCR} . Another axis $j\ V_S/V_R$ is drawn as shown. In this diagram, the positive values of V_S / V_R lie on the left of the vertical axis $j\ V_S/V_R$. Since this is in contrast to the general convention, the curves are transferred on to the plane of the ratio of the relaying signals, S_A and S_B .

Fig.8.3 shows a typical plane of the ratio of the relaying signals. A typical stable zone (vertical shading) is marked on the plane which is obtained by drawing the local end relay characteristic alongwith the inverse of the remote end relay characteristic. The zone of sequential tripping is marked with inclined shading. The rest of the plane represents the zone of simultaneous tripping.

The relay characteristics at the two ends of the line could be of any shape confirming to the following requirements:

(a) There must be a provision of sufficiently large stable zone enclosing the point K= 1 ; δ = 0 well within.

(b) The zone of sequential tripping should be as small as possible and, therefore, the zone of simultaneous tripping as large as possible.

(c) The shape of the characteristic should be as simple as possible so as to be realisable with simple relay circuitry employing minimum number of input signals for the phase or amplitude comparison.

Once the satisfactory shapes of the relay characteristics at the two ends of the line are decided on S_A / S_B plane, they can be transferred back to the respective admittance planes. The comparators employed must be capable of yielding these characteristics on the admittance plane.

It may be noted that in arriving at the proper shape, the local end relay characteristic and the inverse of the remote end relay characteristic are required to be plotted on S_A / S_B plane. Since the inverse of a circle may be a circle or a straight line, and further, its centre and radius (or slope and intercept) on S_A/S_B plane will depend upon the centre and radius (or slope and intercept on one of the axis) of the original characteristic, it would become extremely difficult to select the shape of the stable zone for optimum protection scheme.

In the next section, therefore, an inversion chart is developed which will be found useful in the selection of the appropriate stable zone due to readily determination of the necessary inverse characteristic.

8.4 INVERSION CHART :

The inverse of any characteristic can be found by algebraic methods. However, it will be laborious, and further, when the characteristic under consideration has more discontinuities on the boundary, the method becomes extremely involved. Reference 47 describes the 'inversion chart' useful in finding the inverse of a complex quantity (a point). This chart is modified and drawn in fig.8.4 .

8.4.1 Construction :

Let the equation of the plane bounded by a circle be

$$\left|\frac{S_A}{S_B}\right|_p^2 + \left|\frac{S_A}{S_B}\right|_q^2 + b\left|\frac{S_A}{S_B}\right|_p + C\left|\frac{S_A}{S_B}\right|_q + d \leqslant 0 \quad \ldots(8.2)$$

Where p and q refer to the inphase and quadrature components, and b,c and d are constants. The circle represented by (8.2) has the centre (m,n) given by

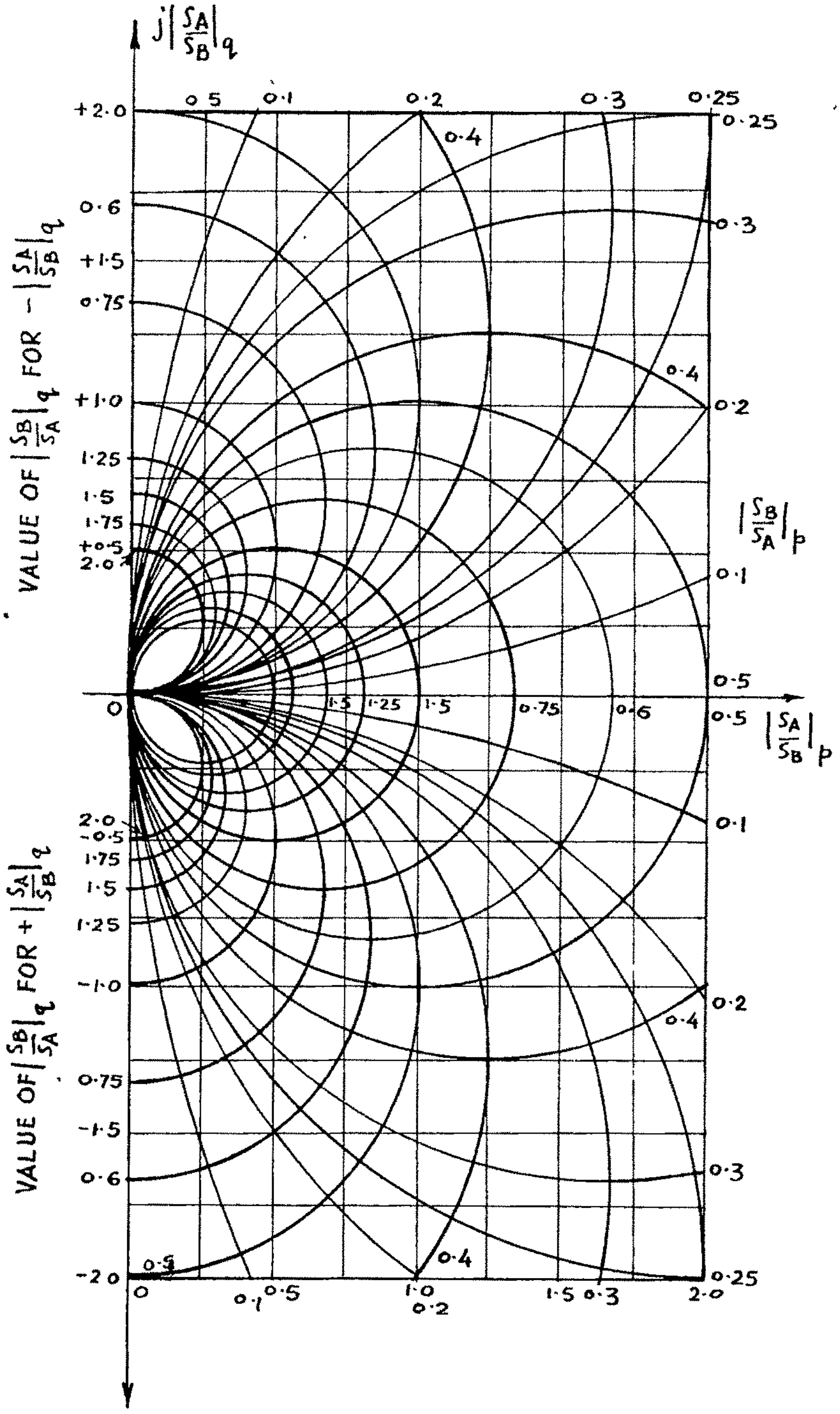

FIG. 8·4 INVERSION CHART

$$m = -\frac{b}{2}, \quad n = -\frac{c}{2} \qquad \ldots. (8.3)$$

If in inequality (8.2) the region of interest is inside the circle and if $d \neq 0$, then the corresponding region of interest of the inverse characteristic can be found referring table 1.

TABLE 1

Sr.No.	Condition	Region of interest
1.	$\frac{m^2 + n^2 - d}{d^2} \leq 0$	Outside the circle
2.	$\frac{m^2 + n^2 - d}{d^2} > 0$	Inside the circle

In the chart of fig.8.4, horizontal and vertical lines are drawn on the S_A / S_B plane with uniform scale. The corresponding inverse are the arcs of circles on the S_B / S_A plane. Each arc is scaled for the corresponding horizontal or vertical straight line.

8.4.2 Method of Use :

In explaining the method of using the chart,it is assumed that identical characteristics are employed at the two ends, which is usually the case.

The characteristic whose inverse is to be found is drawn on S_A/S_B plane. Three convenient points are selected on the boundary of the characteristic. The corresponding values of the points on S_B / S_A plane are noted and plotted on S_A / S_B plane. A circle (or a straight line) is drawn through these three points giving the required inverse characteristic.

8.5 SHAPING OF STABLE ZONE :

In deciding the shape of the stable zone for particular application the three requirements outlined in the previous section must be fulfilled. In view of these requirements typical stable zones are derived employing the inversion chart of fig.8.4 and plotted in fig.8.5.

Fig.8.5(c) illustrates a circular characteristic with centre (1,0) on the S_A / S_B plane. The inverse of this characteristic is also a circle and provides a small region of sequential tripping. Further, the stable zone consisting of arcs of two circles encloses the point $K = 1$; $\delta = 0$ well within due to the large coverage on the S_A / S_B plane. This stable zone can be easily obtained by employing either 2-input amplitude or phase comparator. In fact majority of the relays protecting the linesin this mode employ this stable zone.

The region of sequential tripping of fig.8.5(c) can be further reduced by the superposition of the circle with centre (1/3 ; 0) and radius 1/3 as shown in fig.8.5(d),the latter circle having the blocking tendency outside.

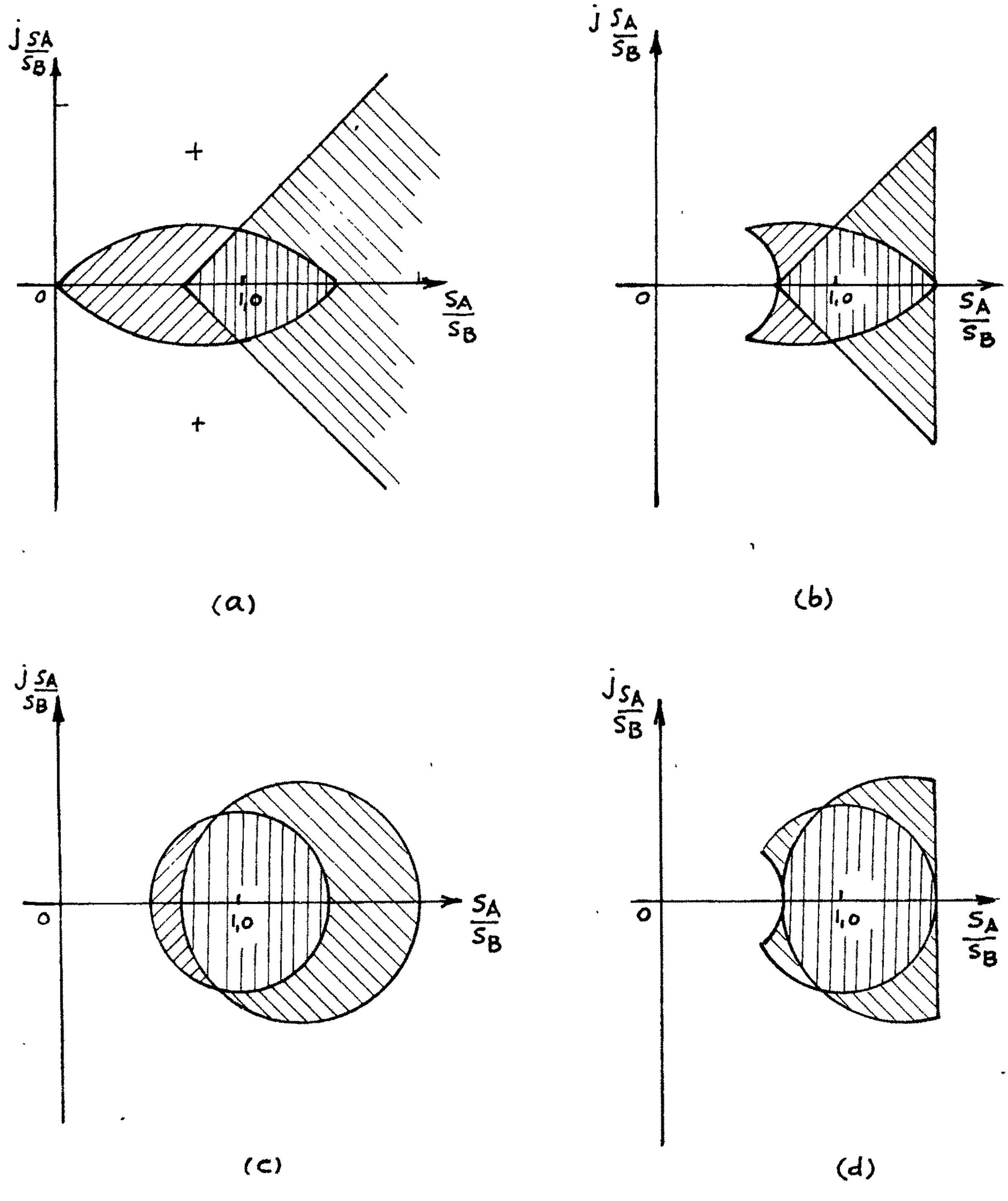

FIG. 8·5 SHAPING OF STABLE ZONE

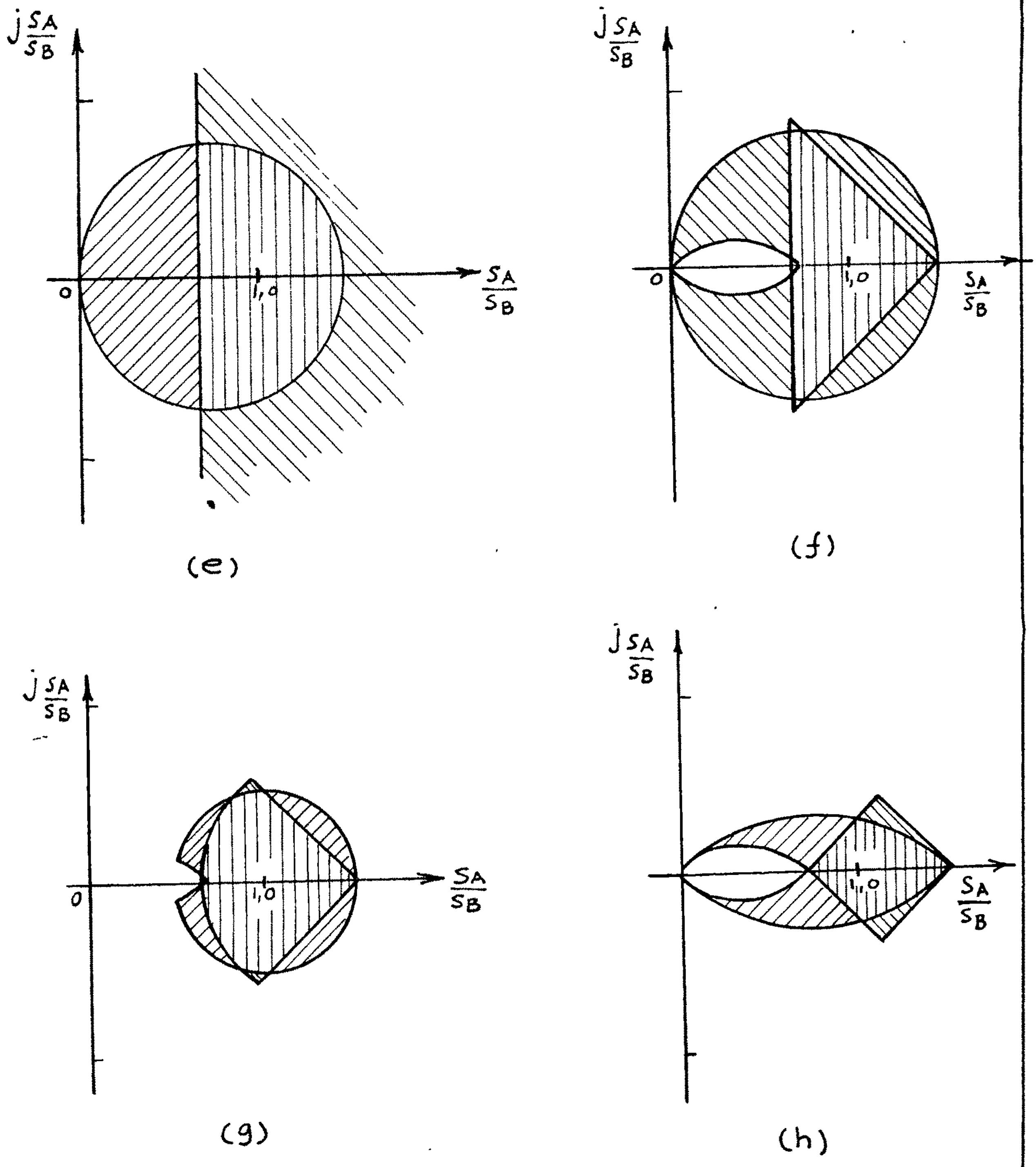

FIG. 8.5 SHAPING OF STABLE ZONE

The stable zone of fig.8.5(a) consists of the straight lines and the arcs of circles. This stable zone can be obtained by employing characteristics consisting of two arcs of circles as shown. The area of sequential tripping in this case, however, is too large which can be reduced by the super-position of the arc of the third circle passing through the origin as shown in fig.8.5(b).

Fig.8.5(e) shows a circular characteristic passing through the origin. It provides a large area of sequential tripping which could be limited by the superposition of the arcs of two circles passing through the origin as shown in fig.8.5(f).

The stable zone of fig.8.5(g) is obtained by two circles similar to those of fig.8.5(f), with the centre of the third circle moved towards the right on the S_A / S_B plane with reduction in its radius. The resulting stable zone provides small region of sequential tripping.

Finally, the stable zone of fig.8.5(h) is obtained by the superposition of four circles, each passing through the origin. The resulting inverse is a quadrilateral.

In fig.8.5 the inverse characteristics can be considered as the original local and remote end characteristics and their inverse as the original characteristics described above. For example, the quadrilateral characteristic of fig.8.5(h) can be considered as the characteristics of the relays at the two ends and their inverse as the resulting region of the arcs of four circles passing through the origin.

The relay circuitry, along with the necessary mathematical back-up, will now be given for both multi-input phase comparator and instantaneous amplitude comparator to obtain some of the typical characteristics of fig.8.5.

8.6 APPLICATION OF SINE TYPE PHASE COMPARATOR :

The sine type comparator will now be analysed for this mode of protection with reference to the stable zone of fig.8.5(b). The mathematical basis of the comparator will be first developed followed by the complete relay circuitry to realise the stable zone. Though this characteristic consists only of arcs of circles, the mathematical basis will be given both for circular as well as rectilinear characteristics for the sake of completeness.

8.6.1 Mathematical Basis Of 2-Input Sine Comparators :

Let the inputs to the 2-input sine comparator be of the form :

$$S_1 = K_1 \angle\alpha_1 \, Y_p \angle\phi_p + C_1 Y_1 \angle\theta_1$$

and

$$S_2 = K_2 \angle\alpha_2 \, Y_p \angle\phi_p + C_2 Y_2 \angle\theta_2 \qquad \text{.... (8.4)}$$

Where $Y_p \angle\phi_p$ is the input admittance of the pilot circuit. $Y_1 \angle\theta_1$ and $Y_2 \angle\theta_2$ are the admittances introduced in the measuring circuits and $K_1 \angle\alpha_1$, $K_2 \angle\alpha_2$, C_1 and C_2 are the constants embracing the term of voltage energizations.

Fig.8.6 illustrates a typical measuring circuit for realising the inputs of eq.(8.4) .

On expressing the signals of eq.(8.4) in the form :

$S_1 = a + jb$

and $S_2 = c + jd$

it can be shown[33] that the condition for the tripping pulse to immerge is ,

$$bc - ad \lessgtr \pm \tan\beta\ (ac + bd) \qquad \ldots\ (8.5)$$

where β accounts for the comparison limits. The sine comparator is set to produce a tripping signal when S_1 leads S_2 . There is no tripping tendency, however, when S_1 lags S_2 .

Substituting (8.4) into (8.5) the latter results in the general condition of tripping as :

$$K_1K_2Y_p^{\,2}\sin(\alpha_1 - \alpha_2) + K_1C_2Y_pY_2\sin(\alpha_1 - \theta_2 + \phi_p)$$
$$+ K_2C_1Y_pY_1\sin(\theta_1 - \phi_p - \alpha_2) + C_1C_2Y_1Y_2\sin(\theta_1 - \theta_2)$$
$$\lessgtr \pm\tan\beta\ [K_1K_2Y_p^2\cos(\alpha_1 - \alpha_2) + K_1C_2Y_pY_2\cos(\alpha_1 - \theta_2 + \phi_p)$$
$$+ K_2C_1Y_1Y_p\cos(\theta_1 - \alpha_2 - \phi_p) + C_1C_2Y_1Y_2\cos(\theta_1 - \theta_2)] \qquad \ldots\ (8.6)$$

The general condition in inequality (8.6) can be written for unsymmetrical comparison limits β_1 and β_2 as ,

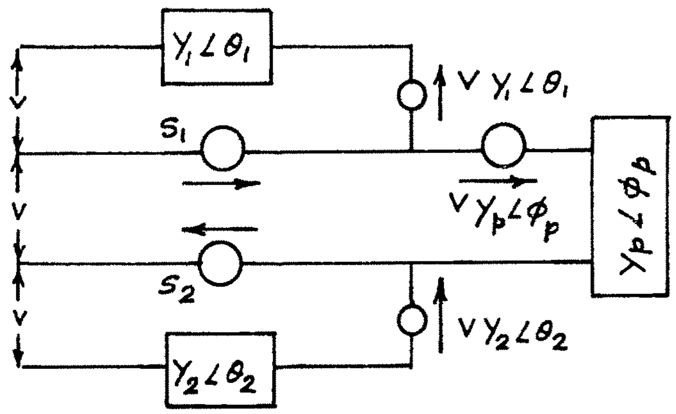

V IS DERIVED FROM THE RELAYING SIGNAL AT THE OUT-PUT OF THE PHASE-CURRENT SUMMATION CIRCUIT.

FIG. 8·6 MEASURING CIRCUIT

$$K_1K_2(G_p^2 + B_p^2)\left[\sin(\alpha_1 - \alpha_2) - \tan\beta_1 \cos(\alpha_1-\alpha_2)\right]$$
$$+ G_p\left[K_2C_1Y_1\left\{\sin(\theta_1 - \alpha_2) - \tan\beta_1\cos(\theta_1 - \alpha_2)\right\}\right.$$
$$\left.+ K_1C_2Y_2\left\{\sin(\alpha_1 - \theta_2) - \tan\beta_1\cos(\alpha_1 - \theta_2)\right\}\right]$$
$$+ B_p\left[K_1C_2Y_2\left\{\cos(\alpha_1 - \theta_2) + \tan\beta_1\sin(\alpha_1 - \theta_2)\right\}\right.$$
$$\left.- K_2C_1Y_1\left\{\cos(\theta_1 - \alpha_2) + \tan\beta_1\sin(\theta_1 - \alpha_2)\right\}\right]$$
$$+ C_1C_2Y_1Y_2\left[\sin(\theta_1-\theta_2) - \tan\beta_1\cos(\theta_1-\theta_2)\right] \leqslant 0 \quad \ldots(8.7)$$

and,

$$K_1K_2(G_p^2 + B_p^2)\left[\sin(\alpha_1-\alpha_2) + \tan\beta_2\cos(\alpha_1-\alpha_2)\right]$$
$$+ G_p\left[K_2C_1Y_1\left\{\sin(\theta_1 - \alpha_2) + \tan\beta_2\cos(\theta_1 - \alpha_2)\right\}\right.$$
$$\left.+ K_1C_2Y_2\left\{\sin(\alpha_1 - \theta_2) + \tan\beta_2\cos(\alpha_1 - \theta_2)\right\}\right]$$
$$+ B_p\left[K_1C_2Y_2\left\{\cos(\alpha_1-\theta_2) - \tan\beta_2\sin(\alpha_1-\theta_2)\right\}\right.$$
$$\left.- K_2C_1Y_1\left\{\cos(\theta_1-\alpha_2) - \tan\beta_2\sin(\theta_1-\alpha_2)\right\}\right]$$
$$+ C_1C_2Y_1Y_2\left[\sin(\theta_1-\theta_2) + \tan\beta_2\cos(\theta_1-\theta_2)\right] \leqslant 0 \quad \ldots(8.8)$$

where
$$\left.\begin{aligned} G_p &= Y_p\cos\phi_p \\ B_p &= Y_p\sin\phi_p \end{aligned}\right\} \quad \ldots\ldots \quad (8.9)$$

In the case of $\beta_1 = \beta_2 = 0$ (comparison limits of π and 2π) inequalities(8.7) and (8.8) reduce to an identical inequality representing a circle with tripping inside if $\alpha_1 > \alpha_2$ and outside if $\alpha_1 < \alpha_2$.

In the case of either one or both β_1 and β_2 being other than zero, inequalities (8.7) and (8.8) must be satisfied simultaneously, the resulting characteristic being the area that is common to both the circles.

8.6.2 Graphical Constructions :

To facilitate the selection of input signals to obtain required stable zone, the graphical constructions will be presented both for rectilinear as well as circular characteristics.

Rectilinear Characteristics :

The inequalities(8.7) and (8.8) will represent rectilinear characteristics if any of the following conditions are employed

$$\begin{aligned} &\text{(i)} \quad K_1 = 0 \; ; \; \alpha_1 = 0 \\ &\text{(ii)} \quad K_2 = 0 \; ; \; \alpha_2 = 0 \end{aligned} \qquad \ldots. (8.10)$$

On substituting $K_1 = -K_1$ and letting $K_2 = 0$; $\alpha_2 = 0$ the inequalities(8.7) and (8.8) reduce to ,

$$B_p \leqslant \tan(\theta_2 - \alpha_1 + \beta_1)\, G_p + \frac{C_1 Y_1}{K_1} \left[\frac{\sin(\theta_1 - \theta_2) - \tan\beta_1 \cos(\theta_1 - \theta_2)}{\cos(\alpha_1 - \theta_2) + \tan\beta_1 \sin(\alpha_1 - \theta_2)} \right] \quad \ldots.(8.11)$$

and,

$$B_p \leqslant \tan(\theta_2 - \alpha_1 - \beta_2)\, G_p + \frac{C_1 Y_1}{K_1}\left[\frac{\sin(\theta_1-\theta_2) + \tan\beta_2 \cos(\theta_1-\theta_2)}{\cos(\alpha_1-\theta_2) - \tan\beta_2 \sin(\alpha_1-\theta_2)}\right] \quad \ldots.(8.12)$$

The graphical construction corresponding to (8.11) and (8.12) is shown in fig.8.7.

Circular Characteristics :

Inequalities(8.7) and (8.8) (with signs of K_1 and K_2 reversed) represent two circles on admittance plane having centres D and E as shown in the graphical construction of fig.8.8. The common region of these two circles is the 'tripping ' region in accordance with inequalities(8.7) and (8.8).

8.6.3 Derivation of Inputs To The Comparator :

In deriving the necessary inputs to the comparator to obtain the characteristic of fig.8.5(b) it is essential to transfer the latter on the admittance plane. Fig.8.9 shows the composite characteristic on the admittance plane.

The arc of the circle O'PQ is obtained employing symmetrical comparison limits,while the arcs RQ and PR are obtained employing unsymmetrical comparison limits to the inputs yielding the circular characteristic RSO'T .

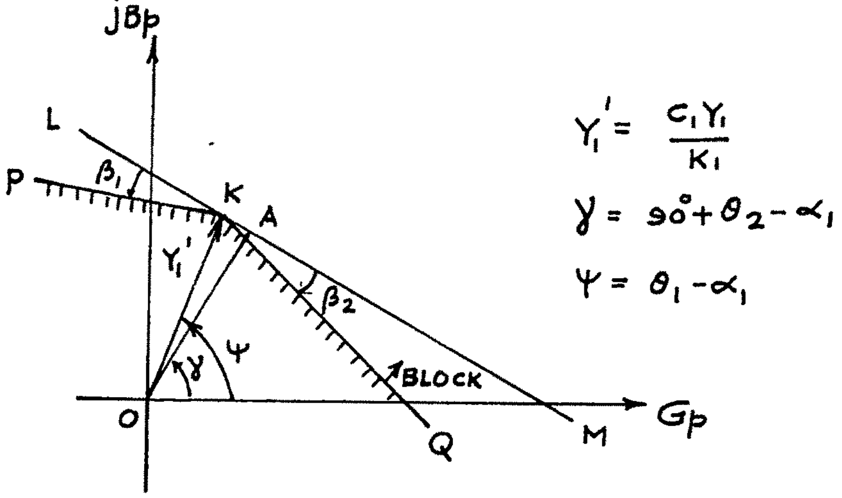

INPUTS

$S_1 = -K_1 \angle\alpha_1 Y_p \angle\phi_p + C_1 Y_1 \angle\theta_1$

$S_2 = C_2 Y_2 \angle\theta_2$

FIG. 8·7 GRAPHICAL CONSTRUCTION - RECTILINEAR CHARACTERISTICS

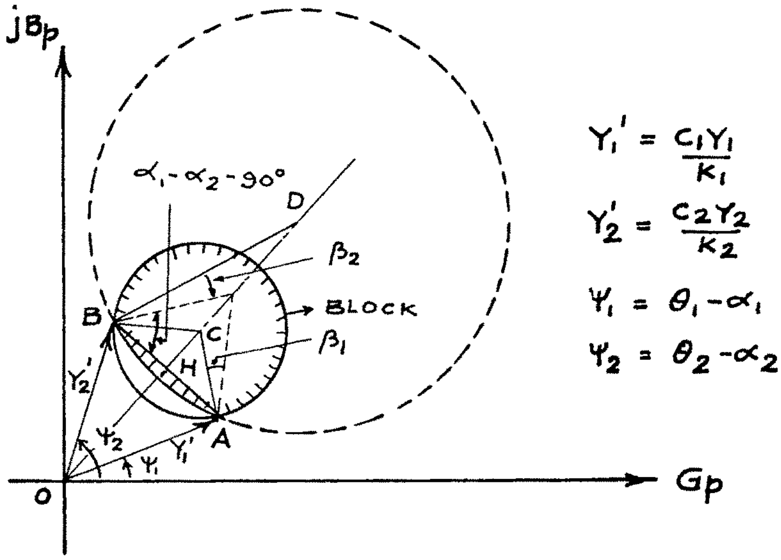

INPUTS

$S_1 = -K_1 \angle\alpha_1 Y_p \angle\phi_p + C_1 Y_1 \angle\theta_1$

$S_2 = -K_2 \angle\alpha_2 Y_p \angle\phi_p + C_2 Y_2 \angle\theta_2$

FIG. 8·8 GRAPHICAL CONSTRUCTION - CIRCULAR CHARACTERISTICS

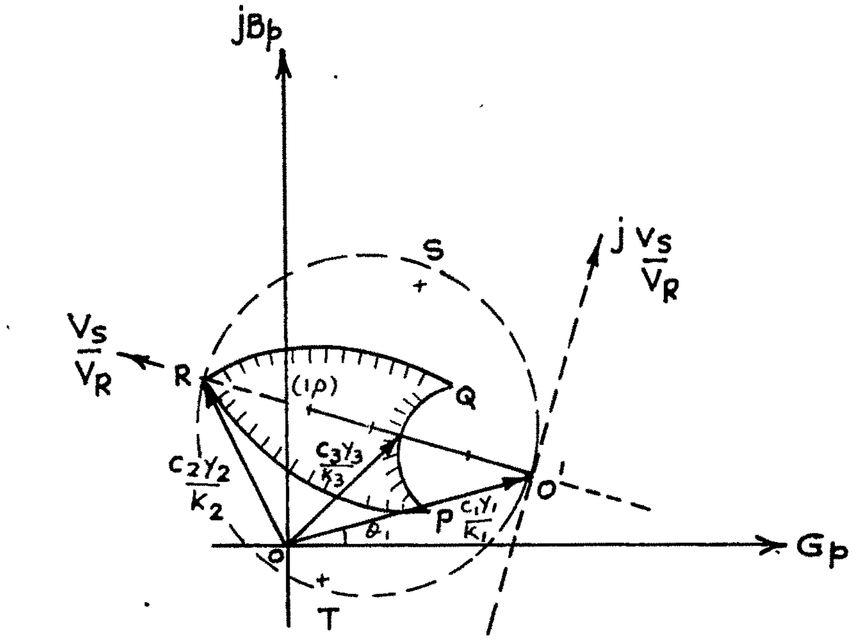

FIG. 8·9 CHACTERISTIC ON ADMITTANCE PLANE

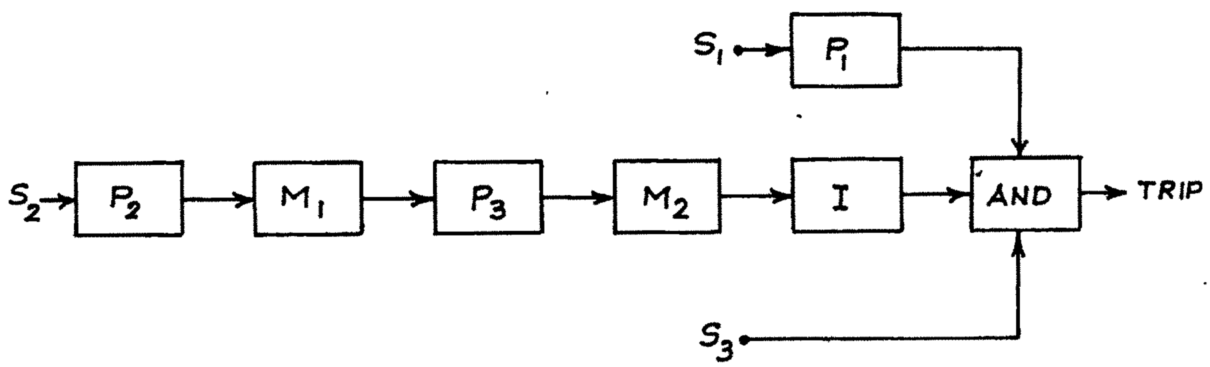

FIG. 8·10 BLOCK-SCHEMATIC DIAGRAM OF THE RELAY

On comparing the characteristic of fig.8.9 with the graphical construction of fig.8.8 following inputs are obtained .

$$
\left.\begin{aligned}
S_1 &= K_1Y_p \angle\phi_p - C_1Y_1\angle\theta_1 \\
S_2 &= K_2 \angle 90^\circ\ Y_p \angle\phi_p + C_2Y_2\angle\theta_2 \\
S_3 &= K_3 \angle -90^\circ\ Y_p \angle\phi_p - C_3Y_3 \angle\theta_3
\end{aligned}\right\} \quad \ldots.(8.13)
$$

Signals S_1 and S_2 are the operating and polarising signals respectively yielding the segments PR and RQ of the characteristic, limits of comparison being β_1 and β_2. Similarly S_1 and S_3 are the operating and polarising signals respectively yielding the segment PQ, limits of comparison being π and 2π .

8.6.4 Relay Circuitry :

It may be noted that in the pairs of signals furnishing the different segments of the characteristic, the operating signal, viz. S_1 , is common. It will, therefore, be possible to employ multi-input phase comparator.

Fig.8.10 illustrates the block-schematic diagram of the relay. The required signals S_1,S_2 and S_3 are obtained from the measuring circuits. A positive going pulse is obtained from S_2 (employing the pulse forming circuit P_2) when the latter changes its sign from negative to positive. This pulse is used to trigger monostable multi-vibrator circuit M_1 set for the comparison limit β_1. A positive going pulse is obtained from the output of M_1(employing the pulse forming circuit P_3) when the latter starts recovering from its quasi-stable state. This pulse is used to trigger monostable multi-vibrator circuit M_3 set for the comparison limit β_2. Invertor circuit I is used to invert the output of M_3 .

A positive going pulse from S_1, obtained by employing the pulse forming circuit P_1, is compared for the phase difference with the output of I and the signal S_3, in the AND gate. The AND gate provides the necessary tripping signal in the form of a pulse which can be used to trigger a thyristor placed in the trip circuit of the circuit breaker rendering the relay completely static.

8.7 APPLICATION OF INSTANTANEOUS AMPLITUDE COMPARATOR :

The quadrilateral characteristic of fig.8.5(h) is considered as the required characteristic. This characteristic is transferred on the admittance plane as shown in fig.8.11.

8.7.1 Principle Of The Comparator :

Fig.8.12 illustrates the basic arrangement of the protective system. Summation transformers at each end of the line are employed to convert 3-phase quantity in to a single phase quantity to facilitate the transmission of information on 2-wire pilot circuit. Replica admittances $Y_1 \angle\theta_1$ and

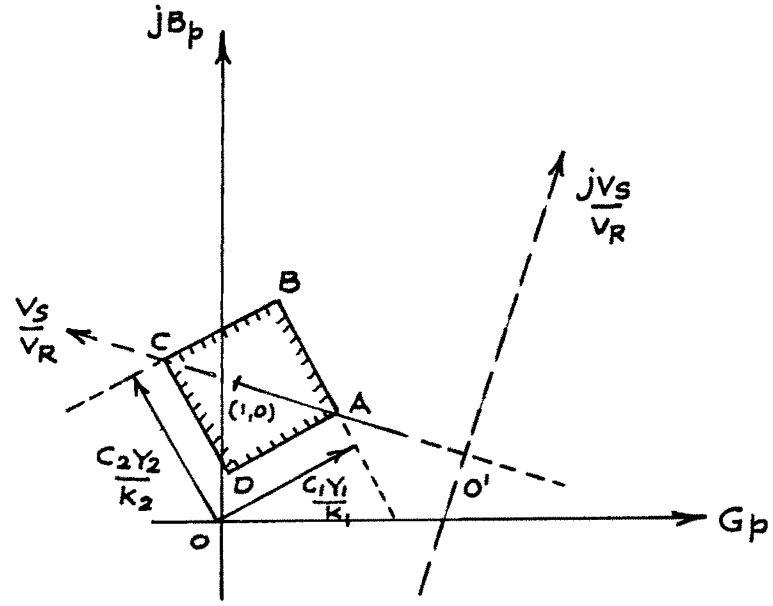

FIG. 8·11 QUADRILATERAL CHARACTERISTIC ON ADMITTANCE PLANE

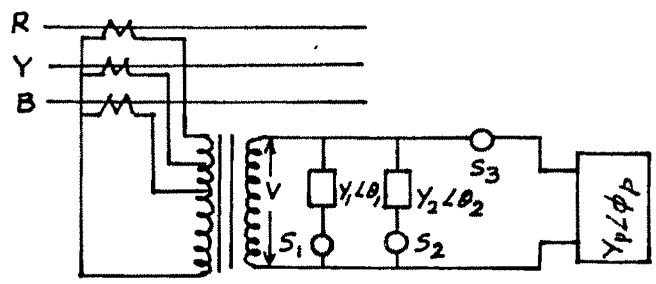

FIG. 8·12 TYPICAL PROTECTIVE ARRANGEMENT

$Y_2 \angle\theta_2$ are introduced to obtain the necessary signals for amplitude comparison given by eq.8.14 .

$$
\left.
\begin{aligned}
S_1 &= C_1Y_1\angle\theta_1 \\
S_2 &= C_2Y_2\angle\theta_2 \\
S_3 &= K_1Y_p \angle\phi_p
\end{aligned}
\right\} \quad \ldots\ldots (8.14)
$$

It may be noted that the signals given by (8.14) are single quantity signals rendering a simple arrangement of the measuring circuit.

Fig.8.13 illustrates the block-schematic diagram of the relay yielding quadrilateral characteristic of fig.8.11. S_1 and S_2 are half wave rectified to assume the operating quantity. S_3 is retained as sinusoidal and is termed as restraining quantity. Through instantaneous comparison of the two quantities, judgement is made continuously of whether or not the operating value is larger than the restraining value.

The operation of the amplitude comparator is best understood by referring to the wave-forms in fig.8.14. A tripping signal is generated when, and only when, the operating quantity is greater than the restraining quantity at every instant during the half-cycle. The comparator circuit is described in section 8.7.2, Fig.8.15 illustrates the necessary Maximum Value selector circuit. It can be easily seen from fig.8.14 that,depending upon the position of S_3, the restraining value for tripping condition is

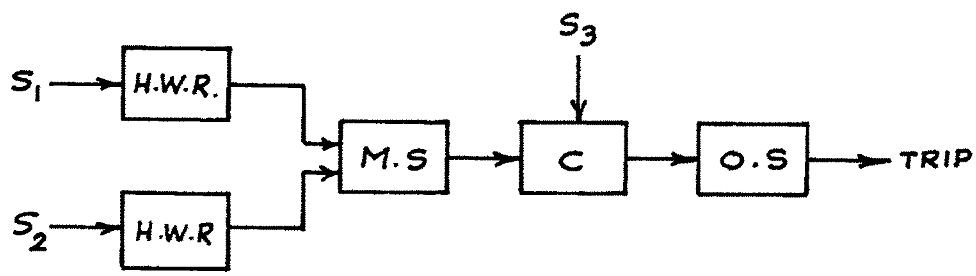

H.W.R. - HALF WAVE RECTIFIER

M.S. - MAXIMUM VALUE SELECTOR

C - INSTANTANEOUS AMPLITUDE COMPARATOR

O.S. - OUT-PUT STAGE

FIG. 8·13 BLOCK-SCHEMATIC DIAGRAM OF THE RELAY

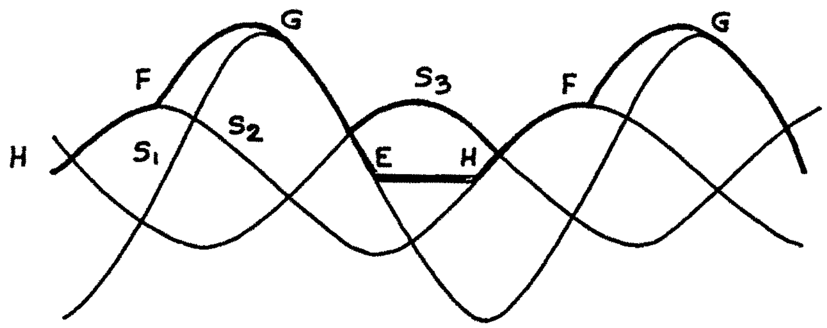

(a) NO OUTPUT PROVIDED

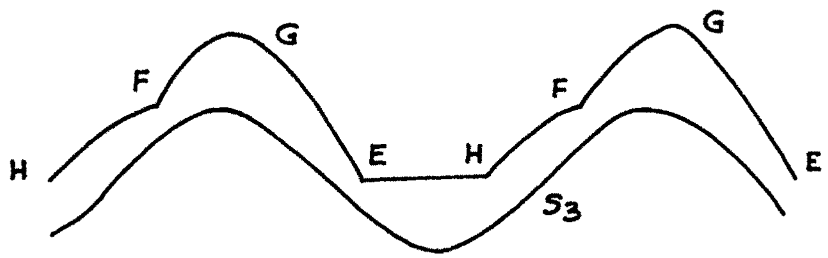

(b) OUTPUT PROVIDED

FIG. 8·14 WAVEFORMS OF THE AMPLITUDE COMPARATOR

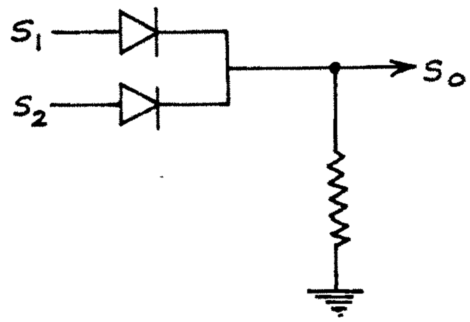

FIG. 8·15 MAXIMUM VALUE SELECTOR

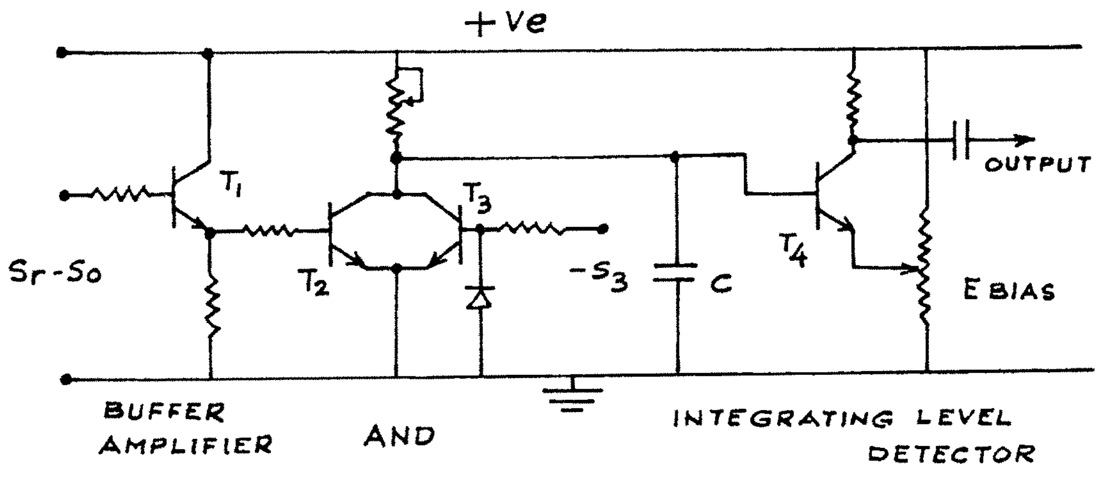

FIG. 8·16 COMPARATOR CIRCUIT

limited by the points E, F, G or H .

When the magnitude of the restraining signal is limited by the point G, with θ_2 greater than θ_1, the operating condition emerges as

$$| K_1 Y_p \sin(\theta_2 - \phi_p) | \leqslant | C_1 Y_1 \sin(\theta_2 - \theta_1) | \quad \ldots. (8.15)$$

or

$$Y_p \leqslant \frac{| C_1 Y_1 \sin(\theta_2 - \theta_1) |}{| K_1 \sin(\theta_2 - \phi_p) |} \quad \ldots. (8.16)$$

where the modulus sign is used to represent the rectified signals and not the average values. Inequality(8.16) represents the line segment AB of the characteristic.

When the magnitude of the restraining signal is limited by the point F, the operating criterion emerges as,

$$| K_1 Y_p \sin(\phi_p - \theta_1) | \leqslant | C_2 Y_2 \sin(\theta_2 - \theta_1) | \quad \ldots(8.17)$$

or

$$Y_p \leqslant \frac{| C_2 Y_2 \sin(\theta_2 - \theta_1) |}{| K_1 \sin(\phi_p - \theta_1) |} \quad \ldots. (8.18)$$

Inequality(8.18) represents the segment BC of the characteristic. The switch-over of the operating characteristic from line AB to line BC occurs when ϕ_p exceeds the angle α obtained by equating (8.16) and (8.18)

i.e. $$\frac{C_1 Y_1 \sin(\theta_2 - \theta_1)}{K_1 \sin(\theta_2 - \alpha)} = \frac{C_2 Y_2 \sin(\theta_2 - \theta_1)}{K_1 \sin(\alpha - \theta_1)} \quad \ldots. (8.19)$$

The simplification of (8.19) yields

$$\alpha = \tan^{-1}\left[\frac{C_1Y_1\sin\theta_1 + C_2Y_2\sin\theta_2}{C_1Y_1\cos\theta_1 + C_2Y_2\cos\theta_2}\right] \qquad \ldots.(8.20)$$

If S_1 and S_2 would have been employed as full wave rectified signals, instead of half-wave rectified, image characteristics of AB and BC would have been present resulting in the formation of the characteristic in the form of a parallalogram enclosing the origin of the admittance plane. However, due to the half-wave rectification only, the image characteristics are eliminated resulting into the overall characteristic of fig.8.11. The segments OC and OA are resulted due to the controlling points E and H (fig.8.14).

It may be observed that the controlling points E,F,G and H, in view of above, produce the tripping tendency of the relay inside the quadrilateral characteristic of fig. 8.11. To make the tripping tendency of the relay outside the characteristic, therefore, a typical output stage is employed which is explained in section 8.7.3.

8.7.2 Comparator Circuit :

The comparator circuit for realising the polar characteristic of fig.8.11 needs special mention. The design of comparator circuit should be such that an output pulse has to be generated only when the operating quantity is greater than the restraining quantity at every instant.

The circuit diagram of the comparator is shown in fig.8.16. The operating and restraining signals are connected in opposition at the base of transistor T_1. E_{bias}, the bias voltage of transistor T_4 is so adjusted that, if C is allowed to charge continuously for half a cycle, T_4 will conduct. Transistor T_3 is fed with the alternating signal $-S_3$. Under normal condition, during one half cycle when $-S_3$ is negative, T_3 stops conducting and allows capacitor C to be charged. During the interval in this half cycle when the restraining quantity is larger than the operating quantity, T_1 conducts making T_2 also conducting and discharges C. In effect the capacitor C is prevented from being charged through a complete half cycle. In the event of the operating quantity becoming larger than the restraining quantity at every instant during the half cycle, T_1 stops conducting making T_2 also stop conducting. C is allowed to charge for a complete half cycle resulting in the output pulse from the level detector.

8.7.3 Output Stage :

It is clear from the foregoing that the level detector in the comparator circuit issues the pulse for admittance vectors occupying the positions inside the quadrilateral characteristic. To invert the sense of tripping, therefore, an output stage is arranged as shown in block-schematic form in fig.8.17.

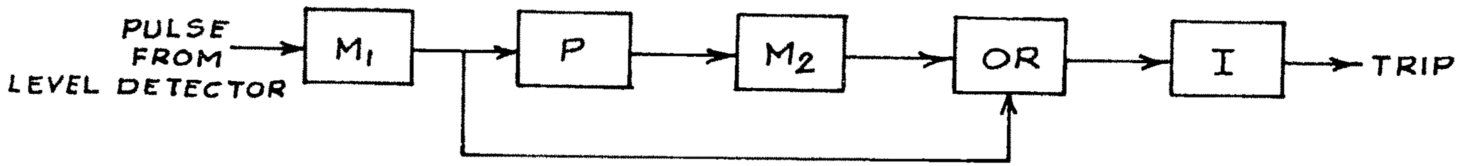

FIG. 8·17 OUT-PUT STAGE IN BLOCK-SCHEMATIC FORM

The pulse from level detector is used to trigger monostable multi-vibrator circuit (M_1) set for almost 3/4th of the cycle. A pulse is obtained from the output of M_1, when the latter starts recovering from its quasi-stable state. This pulse is used to trigger another mono-stable multi-vibrator circuit, M_2, set for similar time delay. The block-output of M_1 and M_2 are OR gated to obtain a continuous wave form.

In the event of the level detector issuing output pulse(blocking condition of the relay), OR gate issues a continuous output block, which on inverting will not issue the tripping signal to the breaker. In the case of legitimate faults in the protected section, level detector will not issue the pulse output. M_1 and M_2,therefore, will not get triggered resulting in the output from the inverting circuit for tripping of the breakers.